Viscous Fingering in a Yield Stress Fluid

Anke Lindner,[1] Philippe Coussot,[2] and Daniel Bonn[1]

[1]*Laboratoire de Physique Statistique, Ecole Normale Supérieure, 24 rue Lhomond, 75231 Paris, France*
[2]*LMSGC, 2 Allée Kepler, 77420 Champs sur Marne, France*

(Received 21 January 2000)

We study the Saffman-Taylor or viscous fingering instability in yield stress fluids. The theory for yield stress fluids shows that the dispersion equation of the instability is similar to that for Newtonian fluids; however, the capillary number governing the instability now contains the yield stress. Experiments using gels and foams reveal very branched fingers in the gel. The results are in excellent agreement with theory for the gel, with, in addition, a crossover from yield stress dominated to viscous behavior. The results for foams are very different due to the existence of wall slip.

PACS numbers: 47.54.+r, 47.20.Gv, 47.20.Hw, 47.50.+d

When a fluid pushes a more viscous fluid in a Hele-Shaw cell, the interface between the two fluids develops an instability leading to the formation of fingerlike patterns, called viscous fingers. This is the so-called Saffman-Taylor instability [1]. For Newtonian fluids, the width w of the viscous fingers is determined by the capillary number $\mathrm{Ca} = \Delta\mu U/\gamma$, the ratio of viscous forces, and capillary forces; $\Delta\mu$ is the viscosity difference between the two fluids, U is the finger velocity, and γ is the surface tension. The viscous forces tend to narrow the finger, whereas the capillary forces tend to widen it: the finger width decreases with increasing Ca. Because of its simplicity, the fingering instability received much attention as an archetype of pattern forming systems and is by now well understood, both experimentally and theoretically [1,2].

A whole different class of problems was uncovered when the instability was studied for non-Newtonian fluids. For such viscoelastic fluids, a wide variety of strikingly different patterns are found [3]. Most natural and industrial materials as, for example, glues, paints, mud, etc., are non-Newtonian. It is thus also from a practical point of view important to understand the instability in such "complex fluids." Experiments using foams, clays, slurries, and polymer gels reveal branched, fractal, or fracturelike patterns [4–8]. The physical origin of the very different structures is so far ill understood, mainly because most of these fluids exhibit multiple viscoelastic characteristics, which were not determined simultaneously. The main mathematical challenge is that the pressure field is no longer Laplacian, making even a numerical prediction of the finger width difficult [9,10].

The examples mentioned above are all believed to exhibit a yield stress: as long as the stress remains below a critical value, they do not flow, but respond elastically to the deformation. This might consequently be at the origin of some of the observed patterns. Theory on yield stress fluids has revealed that the Saffman-Taylor instability is modified drastically [11]. From the theory it can be anticipated that multiple small fingers can propagate in parallel in the channel.

Here we investigate the instability for a polymer gel [12] and a foam [13]. The former shows a yield stress dominated fingering regime for low finger velocities, and a viscous regime for high velocities. The width of the fingers in the yield stress regime is shown to be well described by a linear stability analysis for yield stress fluids. For the foam, however, no such crossover is observed. We show that this is due to the absence of an apparent yield stress because the foam "slips" at the wall.

The experiments are performed in a rectangular Hele-Shaw cell consisting of two glass plates separated by a thin Mylar spacer, fixing the plate spacing b, which can be varied from $b = 0.125$ to 1 mm. The channel width W is 2 or 4 cm. The cell is filled with the fluid; compressed air is used as the less viscous, driving, fluid. The fingers are captured by a CCD camera coupled to a VCR.

For the gel, we find ramified structures for low velocities. One repeatedly observes more than one finger propagating in parallel through the cell for a significant period of time, in agreement with the theory [11]. Eventually one of the fingers will screen the others, which stop moving. The one finger that still moves subsequently destabilizes again, and the whole process starts over. Contrary to what is the case for Newtonian fluids, the width of the finger does not appear to depend on either the propagation velocity or the channel width. However, the finger width does increase with increasing plate spacing (Fig. 1).

For high velocities, a regime is observed in which only a single, stable finger propagates along the center line through the cell. In addition their shape is very similar to that for classical viscous fingers, although their relative finger width $\lambda = w/W$ can be significantly below the limit of $\lambda = 0.5$ found for Newtonian fluids.

To quantify the transition between the low and the high velocity regime, we measure the finger width as a function of the velocity (Fig. 2). As the noise is rather large, the results have been obtained by averaging over several experiments. For low velocities ($U < 0.05$ cm/s) the finger width is indeed independent of the velocity, corresponding to the ramified fingers described above. For

 0031-9007/00/85(2)/314(4)$15.00

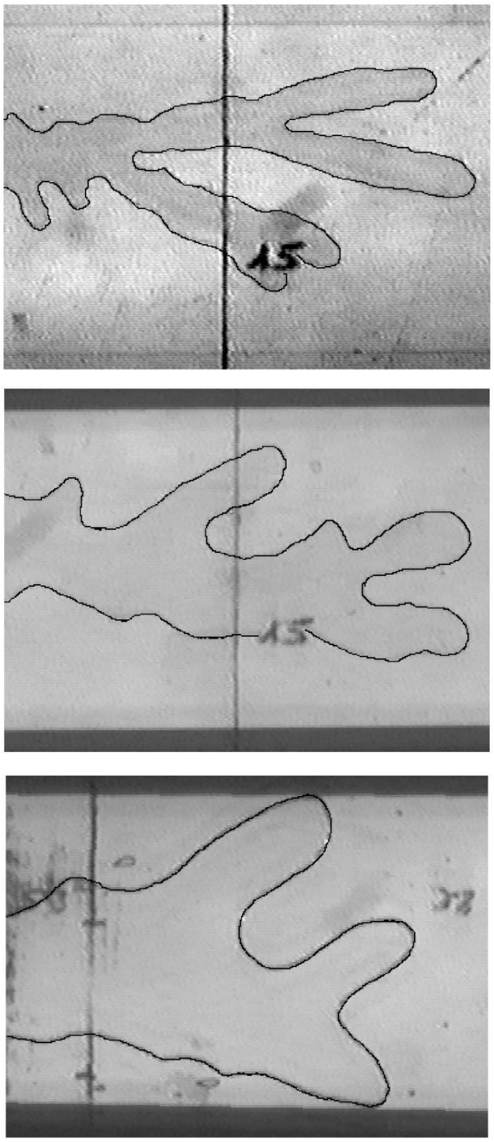

FIG. 1. Snapshots of the viscous fingers for gel at low velocities ($U < 0.01$ cm s) for $W = 4$ cm; plate spacings of $b = 0.125$, 0.25, and 0.75 mm from top to bottom.

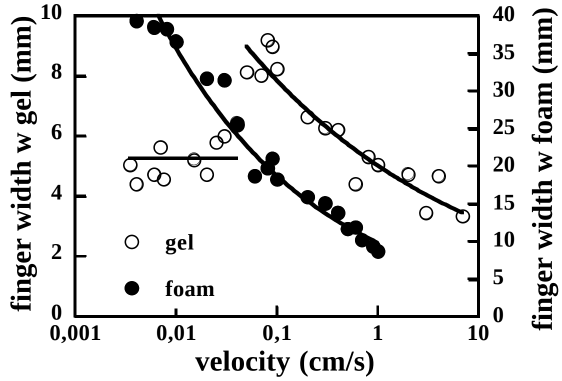

FIG. 2. Finger width versus finger velocity (on a logarithmic scale) for the gel (open circles) and for the foam (filled circles) for $W = 4$ cm and $b = 0.5$ mm.

$U > 0.05$ cm/s, where one finds a single finger in the center line of the cell, the width decreases with increasing U. We thus identify two different regimes. For low velocities, following the motion of air bubbles it seems that flow was almost negligible in some parts of the fluid. The yield point is not exceeded everywhere and the regime is thus referred to as the yield stress regime. This also implies that the finger does not "feel" the presence of the walls delineating the canal in the Hele-Shaw cell, or necessarily the presence of the other fingers that propagate in parallel. This provides an intuitive reason for why multiple fingers can occur. However, in the high velocity, viscous regime the finger "feels" the walls, as it is able to find the center line of the cell.

For the foam, strikingly different results are obtained. No plateau value is found for low velocities and the finger width already decreases with increasing velocity for very low velocities. There is thus no indication of the existence of a yield stress regime (Fig. 2).

The reason for the very different behavior of the two fluids becomes clear when we characterize the rheological behavior of the fluids. This was done on a Reologica Stress-Tech rheometer using a parallel plate geometry (gap 2 mm, diameter 20 mm). The correct way of determining a yield stress [14] is to perform controlled stress tests: one fixes the stress and monitors the shear rate until reaching a steady state. While progressively increasing the stress level, the steady state shear rate suddenly transits from a very small, fluctuating value (about 10^{-5} s^{-1}), which results from residual plasticity and inaccuracy of the apparatus and which does not depend on stress level, to a larger and stable stress-dependent value. For the gel, exactly this behavior was found. In addition, for stresses beyond the yield stress, which were determined by shear rate controlled measurements, the stress (and consequently also the viscosity) varies as a power of the shear rate. Such behavior is usually described by the Herschel-Bulkley [11] model: $\sigma = \sigma_y + \alpha \dot{\gamma}^n$, where σ_y is the yield stress and $\dot{\gamma}$ is the shear rate (Fig. 3).

Surprisingly, the yield stress character of the foam does not show up in the rheological measurements. Visual inspection shows that wall slip occurs when using smooth surfaces of the plate-plate geometry. This leads in the flow curve to a shear-thinning behavior without an apparent yield stress. However, the existence of a yield stress becomes apparent when wall slip is suppressed by gluing sandpaper to both surfaces of the sample cell. A flow curve similar to the one found for the gel is obtained (Fig. 3).

The anomalous behavior of the foam in the Hele-Shaw flow can thus be understood by the fact that the foam slips at the glass plates and consequently moves as a block. The existence of this plug flow is confirmed by the observation that large gas bubbles, which are entrained by the flow, are not deformed. The yield stress of the foam is thus only manifesting itself when the boundaries are modified

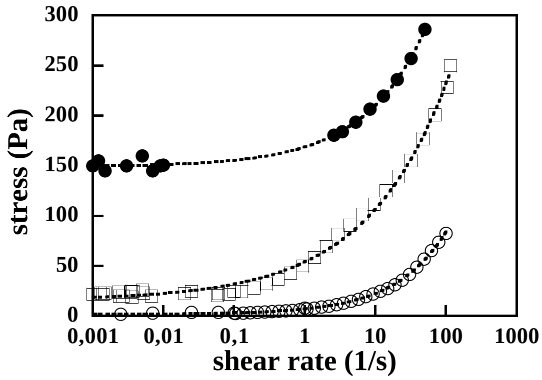

FIG. 3. Rheological measurements of the stress as a function of the shear rate for the gel (□), the foam with a smooth surface (∘) and the foam with a rough surface (•) of the measurement geometry; curves are fits to the Herschel-Bulkley model (gel: $\sigma_y = 16$ Pa, $\alpha = 38$ Pa s^n, $n = 0.38$; foam (rough surface): $\sigma_y = 149$ Pa, $\alpha = 19$ Pa s^n, $n = 0.5$; foam (smooth surface): $\sigma_y = 2$ Pa, $\alpha = 5$ Pa s^n, $n = 0.6$). Fluctuations, probably due to the inaccuracy of the apparatus, made it impossible to obtain reliable results for stresses beyond yield stress for intermediate shear rates, when performing shear rate controlled measurements.

in such a way as to prevent slip at the wall. Thus, to investigate the effect of the yield stress on the Saffman-Taylor instability, we focus on the gel.

Theory for the instability in yield stress fluids has shown that, as is the case for Newtonian fluids, the Saffman-Taylor instability can occur if the yielding fluid (1) is pushed by a less viscous fluid (2) as soon as the wall shear stress difference $\sigma_w = \sigma_{w,1} - \sigma_{w,2}$ is positive. A rigorous theoretical treatment of the Saffman-Taylor instability for a yield stress fluid is complex since the relationship between the velocity and the pressure gradient, the so-called Darcy's law for Newtonian fluids, is no longer linear. Recently, evidence for an effective Darcy's law for shear-thinning liquids in which the viscosity is replaced by the shear-thinning viscosity has been obtained theoretically [10] and experimentally [15]. For the Herschel-Bulkley model described above, it follows that, by analogy, Darcy's law for yield stress fluids can formally be written as $\nabla p = \sigma_w/b = [1 + f(U,b)]\sigma_y/b$, where f is a function such that $f(U) \rightarrow 0$ when the velocity $U \rightarrow 0$. It was shown that approximate expressions for f may be found from the expression for the discharge rate [11].

By using this effective Darcy's law, a linear stability analysis of the flat interface can be performed. It was demonstrated [11] that the dispersion equation is in fact very similar to the Newtonian case. In the Newtonian case the wavelength of maximum growth is given by $\lambda_m = 2\pi\sqrt{\gamma b^2/\mu U}$ [16], where $\mu U/b \simeq \mu\dot{\gamma}$ represents a characteristic viscous stress. For yield stress fluids, the viscous stress should be replaced by the wall shear stress σ_w. Neglecting the air viscosity (and thus $\sigma_{w,2}$) the wavelength of maximum growth is then simply found from the ratio of the capillary forces to the total viscous forces, which now include the yield stress, and follows as $\lambda_m = 2\pi\sqrt{3\gamma b/(2\sigma_w)}$.

This has a number of interesting consequences. The result shows that the wavelength remains finite even at vanishing velocities simply because σ_w contains the finite yield stress. It also explains why for low velocities, for which the yield stress dominates, the finger width, which at least shortly after destabilization should correspond to the wavelength of maximum growth, is independent of the velocity. The other consequences are that the finger width should scale as the square root of the plate spacing and be independent of the channel width.

In order to test the predictions, the finger width was measured varying the plate spacing b from 0.125 mm to 1 mm for channel widths of $W = 2$ cm and $W = 4$ cm, respectively. The results in the yield stress regime are depicted in Fig. 4, where the average finger width w is given as a function of $\sqrt{b}$. Indeed, the finger width shows the dependence on the channel geometry predicted by the theory. More quantitatively, one can obtain the yield stress from the slope of the line, when equating σ_w to the yield stress and identifying the finger width with $\lambda_m/2$. If these identifications are made, one obtains $\sigma_y = 15.6$ Pa, in good agreement with the value $\sigma_y = 16 \pm 2$ Pa obtained independently from the rheological measurements. The simple theory thus does very well in describing the data.

To test the generality of the results, an oil in water emulsion [17] was used as a second yield stress fluid. Very similar behavior with respect to the gel is observed (Fig. 4). The experimentally determined yield stress for the emulsion is somewhat higher than that for the gel; in qualitative agreement, λ_m is found to be somewhat smaller. More quantitatively, from the slope, one finds $\sigma_y = 20$ Pa, whereas the rheological measurements give $\sigma_y = 25 \pm 5$ Pa. Note that the yield stress for the emulsion is more difficult to measure with regard to the gel due to the higher viscosity of the latter.

For the viscous regime, at higher velocities, the viscous stress overcomes the yield stress and the fluid should

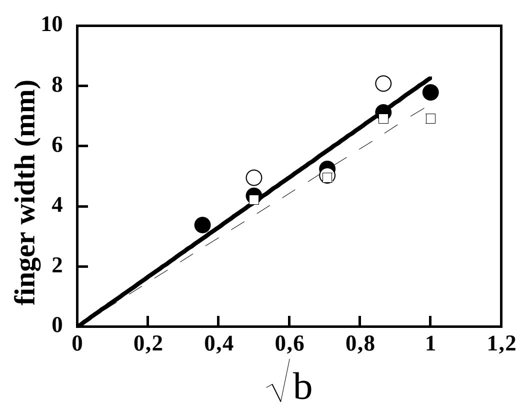

FIG. 4. Finger width versus $\sqrt{b}$ for channel widths of 4 cm (•) and 2 cm (∘) for the gel and for the emulsion (□) for $W = 4$ cm.

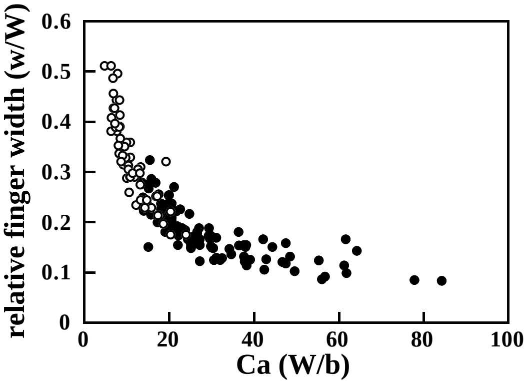

FIG. 5. Relative finger width as a function of Ca(W/b) for channel widths of $W = 4$ (•) and 2 cm (∘) and plate spacings of $b = 0.125$, 0.25, 0.5, 0.75, and 1 mm.

behave like an ordinary viscous fluid which exhibits shear thinning. From Fig. 2, one observes that the finger width λ in this regime decreases with increasing finger velocity. In addition, for high velocities, λ turns out to be much smaller than the classical limit $\lambda = 0.5$. Similar results have already been found for other shear-thinning fluids, such as polymer solutions [15].

For Newtonian fluids, the control parameter allowing one to rescale experiments for different fluids and aspect ratios of the Hele-Shaw cell onto a single, universal curve is $1/B = \mathrm{Ca}(W/b)^2$ [1]. This follows classically from comparing the channel width W to λ_m: $1/B = (2\pi W/\lambda_m)^2$. We have shown recently that for weakly shear-thinning fluids the same rescaling can be applied, provided the viscosity is replaced by the shear-thinning viscosity [15]. However, for the gel, the power index n of the Herschel-Bulkley model is found to be 0.38, which corresponds to a rather strong shear-thinning behavior: the results do not collapse onto a single curve. Surprisingly, it is possible to obtain a very satisfactory data collapse by scaling on Ca(W/b) rather than $1/B$ (Fig. 5). This shows that either the dependence on Ca is stronger or the dependence on W/b is weaker than for the Newtonian case. Although we have been unable so far to find a satisfactory explanation for this nevertheless convincing rescaling of the data, it is worthwhile noting that due to the modification of Darcy's law the dependence of λ_m on b is weaker for yield stress fluids, which leads to a modification of $1/B$. However this cannot account completely for the scaling, as the dependence on W is not modified. This suggests that 3D effects may become important.

In conclusion, we have demonstrated that the Saffman-Taylor instability is drastically modified in yield stress fluids, leading to very branched patterns at low velocity, where the yield stress plays an important role. The results in the yield stress regime can be understood quantitatively from a linear stability analysis. For higher velocities only a single stable finger is observed. Fractal patterns also observed in yield stress fluids [4–8] occur as secondary instabilities at high speeds, for which the viscous stresses dominate the yield stress: these are thus probably not related to the yield stress character of the fluid. The results for the foam indicate that wall slip strongly influences the instability, a point that is also very important if one wants to compare results for different yield stress fluids.

We thank Jacques Meunier, H. Kellay, and M. Ben Amar for helpful discussions. LPS de l'ENS is UMR 8550 of the CNRS, associated with the Universities Paris 6 and Paris 7. LMSGC is UMR113 LCPC-CNRS. A. L. was supported by the DAAD under the HSP III.

[1] P. G. Saffman and G. I. Taylor, Proc. R. Soc. A **245**, 312 (1958); J. W. McLean and P. G. Saffman, J. Fluid Mech. **102**, 455 (1981).
[2] D. Bensimon, L. P. Kadanoff, S. Liang, B. I. Shraiman, and C. Tang, Rev. Mod. Phys. **58**, 977 (1986); G. M. Homsy, Annu. Rev. Fluid Mech. **19**, 271 (1987); Y. Couder, *Chaos, Order and Patterns,* edited by R. Artuso *et al.* (Plenum, New York, 1991).
[3] K. V. McCloud and J. V. Maher, Phys. Rep. **260**, 139 (1995).
[4] H. Van Damme, E. Lemaire, O. M. Abdelhaye, A. Mourchid, and P. Levitz, *Non-linearity and Breakdown in Soft Condensed Matter,* edited by K. K. Bardan *et al.,* Lecture Notes in Physics Vol. 437, (Springer, New York, 1994).
[5] E. Lemaire, P. Levitz, G. Daccord, and H. VanDamme, Phys. Rev. Lett. **67**, 2009 (1991).
[6] J. Nittmann, G. Daccord, and H. E. Stanley, Nature (London) **314**, 141 (1985).
[7] S. S. Park and D. J. Durian, Phys. Rev. Lett. **72**, 3347 (1994).
[8] H. Zhao and J. V. Maher, Phys. Rev. E **47**, 4278 (1993).
[9] M. Ben Amar, Phys. Rev. E **51**, 3819 (1995); E. Corvera Poiré and M. Ben Amar, Phys. Rev. Lett. **81**, 2048 (1998).
[10] L. Kondic, M. J. Shelley, and P. Palffy-Muhoray, Phys. Rev. Lett. **80**, 1433 (1998); L. Kondic, P. Palffy-Muhoray, and M. J. Shelley, Phys. Rev. E **54**, R4536 (1996).
[11] P. Coussot, J. Fluid Mech. **380**, 63 (1999).
[12] Commercial hair gel (Miss Helen, blue).
[13] Commercial shaving foam (Gilette Foamy, regular).
[14] P. Coussot and C. Ancey, *Rheophysics of Pastes and Suspensions* (EDP Sciences, Paris, 1999) (in French).
[15] A. Lindner, D. Bonn, and J. Meunier, Phys. Fluids **12**, 256 (2000).
[16] R. L. Chuoke, P. van Meurs, and V. Van der Pol, Pet. Trans. AIME **216**, 188 (1959).
[17] A commercial day cream (Diadermine, Henkel).